High-Speed Shaft Bearing Loads Testing and Modeling in the NREL Gearbox Reliability Collaborative

Preprint

B. McNiff
McNiff Light Industry

Y. Guo, J. Keller, and L. Sethuraman
National Renewable Energy Laboratory

NOTICE

The submitted manuscript has been offered by an employee of the Alliance for Sustainable Energy, LLC (Alliance), a contractor of the US Government under Contract No. DE-AC36-08GO28308. Accordingly, the US Government and Alliance retain a nonexclusive royalty-free license to publish or reproduce the published form of this contribution, or allow others to do so, for US Government purposes.

This report was prepared as an account of work sponsored by an agency of the United States government. Neither the United States government nor any agency thereof, nor any of their employees, makes any warranty, express or implied, or assumes any legal liability or responsibility for the accuracy, completeness, or usefulness of any information, apparatus, product, or process disclosed, or represents that its use would not infringe privately owned rights. Reference herein to any specific commercial product, process, or service by trade name, trademark, manufacturer, or otherwise does not necessarily constitute or imply its endorsement, recommendation, or favoring by the United States government or any agency thereof. The views and opinions of authors expressed herein do not necessarily state or reflect those of the United States government or any agency thereof.

This report is available at no cost from the National Renewable Energy Laboratory (NREL) at www.nrel.gov/publications.

Available electronically at http://www.osti.gov/scitech

Available for a processing fee to U.S. Department of Energy and its contractors, in paper, from:

    U.S. Department of Energy
    Office of Scientific and Technical Information
    P.O. Box 62
    Oak Ridge, TN 37831-0062
    phone: 865.576.8401
    fax: 865.576.5728
    email: mailto:reports@adonis.osti.gov

Available for sale to the public, in paper, from:

    U.S. Department of Commerce
    National Technical Information Service
    5285 Port Royal Road
    Springfield, VA 22161
    phone: 800.553.6847
    fax: 703.605.6900
    email: orders@ntis.fedworld.gov
    online ordering: http://www.ntis.gov/help/ordermethods.aspx

Acknowledgment

Executive Summary

Bearing failures in the high-speed output stage of the gearbox are a leading cause of unscheduled maintenance in wind turbines. Accordingly, the National Renewable Energy Laboratory (NREL) Gearbox Reliability Collaborative (GRC) has performed an experimental and theoretical investigation of loads within these bearings. The purpose of this paper is to describe the instrumentation, calibrations, data post-processing, and initial results from this testing and modeling effort. Efforts to relate high-speed shaft (HSS) torque, bending, and bearing loads to model predictions are also discussed in this work. Of additional interest is examining whether the shaft measurements can be simply related to bearing load measurements, eliminating the need for making invasive modifications to the bearing races to accommodate such instrumentation.

Table of Contents

List of Figures

1 Introduction

Since 2007, the NREL GRC has been investigating internal and external gearbox motion, loads, and deflections through modeling, analysis, and full-scale field and dynamometer testing. GRC Phases 1 and 2 focused primarily on acquiring measurements in the planetary sections of two 750-kilowatt (kW) test gearboxes (Link et al. 2011).

Feedback from GRC partners highlighted the need for measurements of gear and bearing response on the high speed shaft (HSS) locating tapered roller bearing (TRB) pair, because of the high rate of failures and subsequent repair costs for these bearings in the industry (Sheng 2013, Scott et al. 2012). The reliability of this bearing configuration remains a weak link owing to a possible disconnect between the actual loading behavior, and the loading behavior assumed by the design. HSS bearings can be subject to low loads at high speeds, torque transients, and even torque reversals. When rollers enter and leave the shifting load zone during such events, bearings are prone to skidding, which leads to surface distress and damage (Jain and Hunt 2011).

In GRC Phase 3, instrumentation was added to measure the HSS bending, torque, pinion tooth load distribution, and radial load distribution and temperature of the locating TRBs. The current dynamometer test program measures these loads during normal operation with nontorque rotor loads, generator misalignment, and transient operation (Link et al. 2012). In this report, the experimental HSS measurements are compared to an analytical model and a SIMPACK multibody model.

1

2 Test Summary

The 2.5-megawatt dynamometer test facility at the National Wind Technology Center enabled researchers to apply loads to the GRC drivetrain under controlled, field-like conditions. The following sections summarize the instrumentation and testing of the GRC drivetrain and HSS.

2.1 Instrumentation

The GRC HSS is supported by a cylindrical roller bearing (CRB) upwind, and a close-coupled 32222 J2 TRB pair mounted in an O-configuration downwind of the gear mesh. As shown in Figure 1, orthogonal shaft bending moments were measured using full-bridge strain gauge arrangements mounted downwind (location A) and upwind (location B) of the gear mesh, and also downwind of the TRB pair (location C) where torque was also measured. Bearing loads were measured using Poisson half-bridge strain gauge arrangements installed in machined slots on the outer race of each TRB at two different axial locations in four circumferential positions (Link et al. 2012, Keller and McNiff 2014).

2.2 Calibration

The shaft torque, bending, and TRB signals were calibrated to obtain the conversion coefficients between measured voltages and engineering units of loads for direct comparison against predictions from modeling tools. The calibration coefficients for shaft bending moments and torque were obtained and verified by static in-situ calibration (Keller and McNiff 2014), and a special test rig was used for calibration of the TRB gauges (Keller et al. 2013).

2.3 Dynamometer Testing

The current test program includes a broad matrix of operations to identify those that result in anomalous HSS responses; however, for this work, the drivetrain was operated at full speed (1800 revolutions per minute on the HSS) and at power levels up to 100% (750 kW) in torque-only conditions. HSS data were acquired at 2 kilohertz for 1 second (30 shaft revolutions).

3 Modeling and Analysis Approach

This section presents the analytic model used to estimate TRB loads from measured shaft bending moments and torque, along with a description of the SIMPACK model.

3.1 Bearing Forces From Analytical Model

This section presents the analytical model developed to derive unknown CRB and TRB loads from measured shaft bending moments and torque. If validated, this analytical model would preclude the need for invasive instrumentation on the TRBs. In this model, the HSS is supported by the generator coupling and three bearings, which are treated as unknowns and are determined by solving the force and moment equations satisfying static equilibrium. The free-body diagram of the HSS is shown in Figure 1.
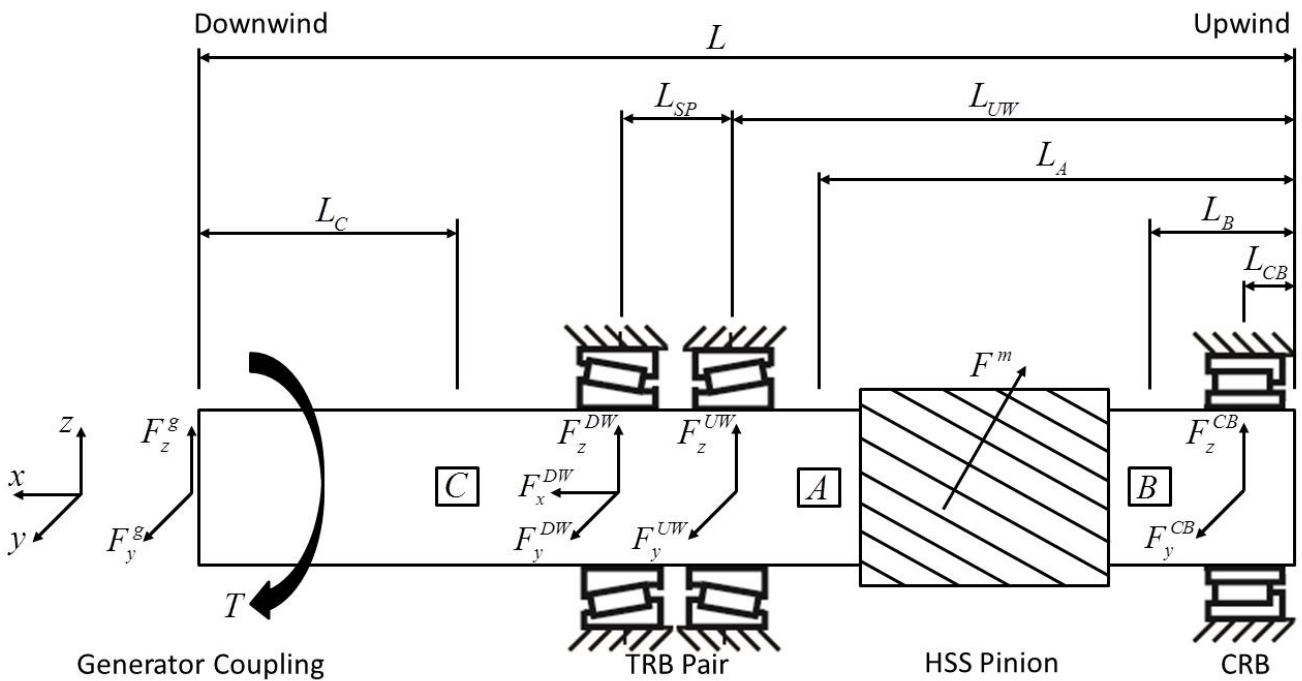
Figure 1. HSS free-body diagram

The following assumptions were made in developing the free-body diagram:

- The shaft is rigid and its weight is negligible

- The CRB does not carry a bending moment or react to axial force

- The upwind TRB does not carry axial load

- The TRBs do not carry bending moments, because their radial stiffnesses are much greater than their tilting stiffnesses

- The generator coupling does not transmit moments or axial force.

3

These assumptions are anticipated to be valid during normal operating conditions, but may be inappropriate when significant shaft misalignment is present. Writing the force balance equations in three directions, moment balance in two directions at three locations, and torque in equilibrium yields ten equations to solve for the ten unknowns in terms of HSS geometric properties and measured shaft bending and torque yields:

$$F^m = \frac{T}{R\cos\beta} \tag{1}$$

$$F_y^g = -\frac{M_z^C}{L_C} \tag{2}$$

$$F_z^g = +\frac{M_y^C}{L_C} \tag{3}$$

$$F_y^{CB} = +\frac{M_z^B}{L_B - L_{CB}} \tag{4}$$

$$F_z^{CB} = -\frac{M_y^B}{L_B - L_{CB}} \tag{5}$$

$$F_y^{UW} = \frac{1}{L_{SP}}\left[-\frac{M_z^C}{L_C}(L - L_{SP} - L_{UW}) + M_z^A - \frac{T}{R}\sin\alpha(L_{SP} + L_{UW} - L_A) \right. \\ \left. -\frac{M_z^B}{L_B - L_{CB}}(L_{SP} + L_{UW} - L_A)\right] \tag{6}$$

$$F_z^{UW} = \frac{1}{L_{SP}}\left[+\frac{M_y^C}{L_C}(L - L_{SP} - L_{UW}) - M_y^A - \frac{T}{R}\cos\alpha(L_{SP} + L_{UW} - L_A) \right. \\ \left. +\frac{M_y^B}{L_B - L_{CB}}(L_{SP} + L_{UW} - L_A)\right] \tag{7}$$

$$F_x^{DW} = \frac{T}{R}\tan\beta \tag{8}$$

$$F_y^{DW} = \frac{1}{L_{SP}}\left[+\frac{M_z^C}{L_C}(L - L_{UW}) - M_z^A + \frac{T}{R}\sin\alpha(L_{UW} - L_A) \right. \\ \left. +\frac{M_z^B}{L_B - L_{CB}}(L_{UW} - L_A)\right] \tag{9}$$

$$F_z^{DW} = \frac{1}{L_{SP}}\left[-\frac{M_y^C}{L_C}(L - L_{UW}) + M_y^A + \frac{T}{R}\cos\alpha(L_{UW} - L_A)z \right. \\ \left. -\frac{M_y^B}{L_B - L_{CB}}(L_{UW} - L_A)\right] \tag{10}$$

4

In this formulation, R, α, and β are the pitch diameter, the angle between the line of action and the z axis, and helix angle. The properties of the GRC HSS are: $L = 775$ mm, $R = 57$ mm, $\alpha = 10º$, and $\beta = 14º$. The bearing locations are $L_{CB} = 33.5$ millimeters (mm), $L_{UW} = 333.5$ mm, and $L_{SP} = 79$ mm. The instrumentation locations are $L_A = 260.5$ mm, $L_B = 88.5$ mm, $L_C = 298$ mm (Keller and McNiff 2014).

3.2 Bearing Forces From SIMPACK Model

A multibody model of the GRC drivetrain was created in SIMPACK to simulate the dynamometer test (Guo et al. 2014). The HSS bearings were modeled as six-axial elastokinematic force elements, which follow a force-displacement relationship based on known stiffnesses and clearances. The bearing stiffnesses were calculated from RomaxWIND at rated torque, accounting for a 5-mm HSS axial offset (Keller and McNiff 2014) and assuming zero TRB preload. The axial stiffness of the upwind TRB was then assumed to be zero. SIMPACK solved the equations of motion by time integration and provided a time history of bearing forces. The bearing internal load distributions cannot be obtained from SIMPACK; instead, they will be the subject of future study using other tools.

5

4 Results

The following sections compare the tests first to the SIMPACK model, and then to the analytic model. All cases were at rated torque and zero nontorque load.

4.1 Shaft Bending and Torque Correlation

Figure 2 compares the measured shaft torque and bending moment measurements to those predicted by SIMPACK. Generally, the results compared very favorably with the largest disparity at the location downwind of the TRB pair (location C). However, the moments at this location were very low in magnitude compared to those at either side of the gear mesh (locations A and B). Although the generator was aligned prior to testing, some generator misalignment could have resulted in the disparity at location C.
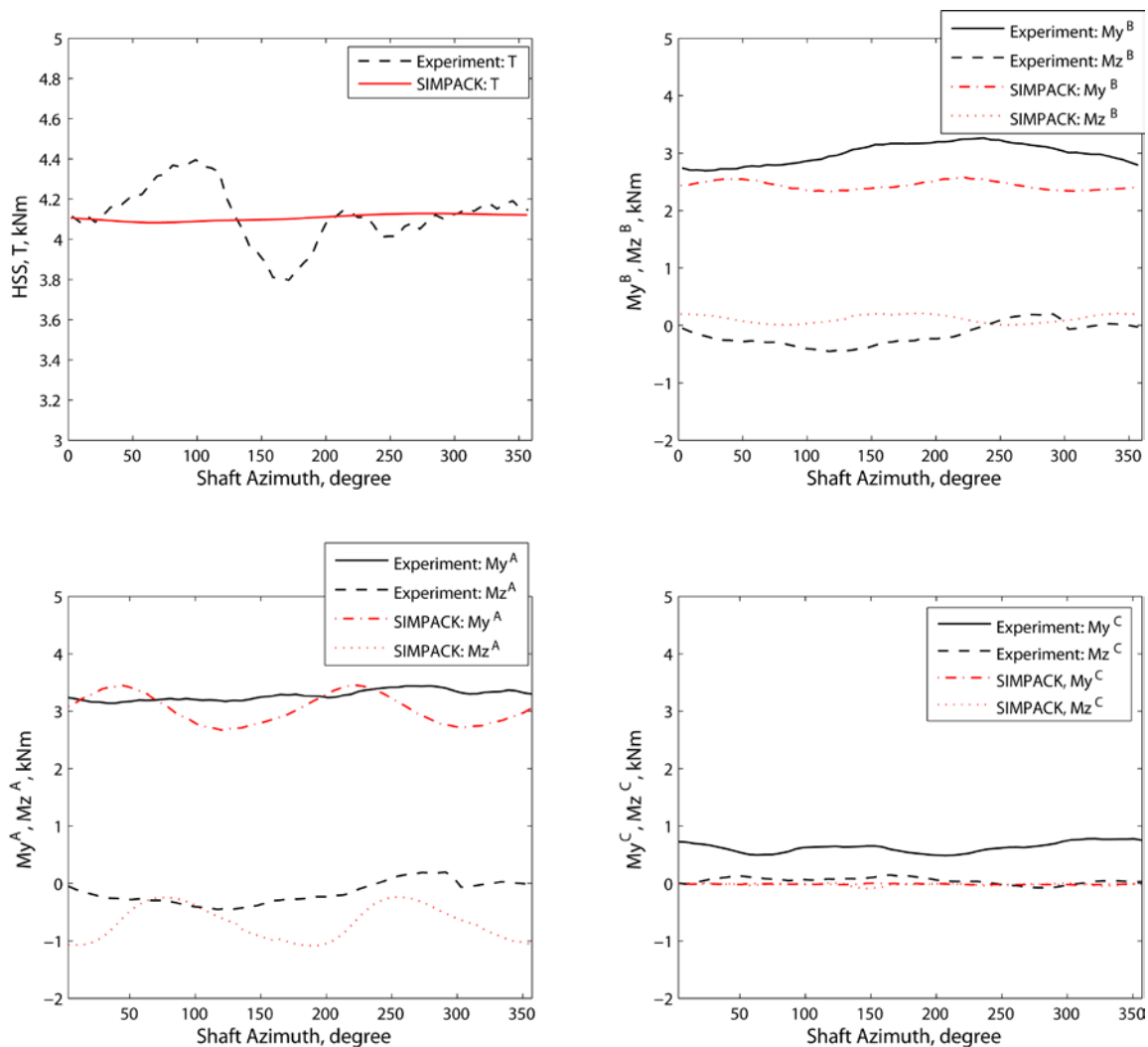

Figure 2. Comparison of measured and SIMPACK-predicted HSS bending moments

4.2 Estimation of Global TRB Loads From Bearing Measurements

Figure 3 shows the measured TRB loads and estimated load zones. Each TRB slot has two gauges in the axial direction, the measurements of which were averaged into one value. The resulting four average circumferential points were then used to describe the load zone, which was assumed to be circular. Other load zone fits will be the subject of future study. The resultant global bearing force vector was then obtained by integrating the load zone.

The upwind bearing has only a few rollers in contact whereas all downwind bearing rollers carry load. The load sharing between these rows was clearly unequal. One possible reason is that the TRB pair was designed with essentially zero preload and mistakenly manufactured with no axial upwind restraint. In this situation, the HSS gear mesh force unloaded the upwind TRB (Keller and McNiff 2014).
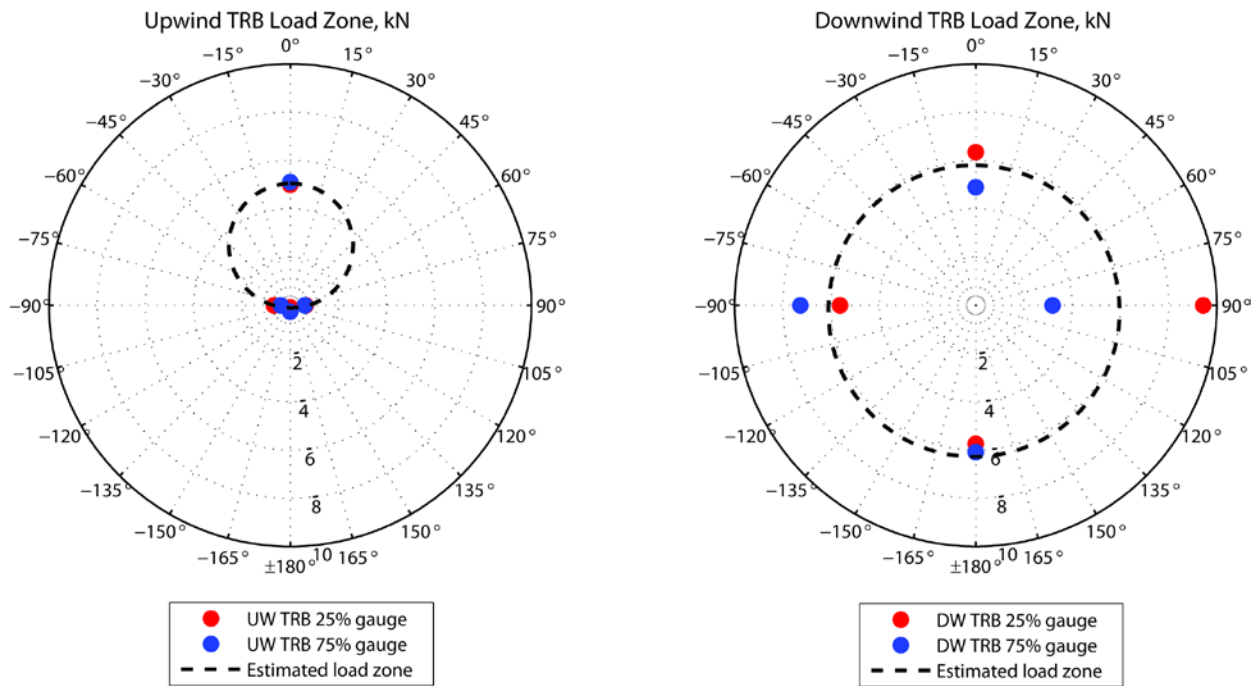

Figure 3. Measured TRB load zone at rated torque

Figure 4 compares the direct TRB load measurements, derived as described above, to the SIMPACK model predictions. Additionally, the measured shaft bending and torque were used to estimate the TRB loads using the analytic model described in equations 6 to 10. The downwind TRB axial load was plotted directly in Figure 4, and the y and z axis loads for both bearings were combined into a single radial load, calculated as $F_r^{DW} = \sqrt{\left(F_y^{DW}\right)^2 + (F_z^{DW})^2}$ and $F_r^{UW} = \sqrt{\left(F_y^{UW}\right)^2 + (F_z^{UW})^2}$. Both SIMPACK and the analytical method assumed that the upwind TRB axial load was zero.

There was very good agreement between the SIMPACK model and the analytical model for the downwind TRB axial load, each having a value of approximately 18 kN. The direct measurement, however, was only approximately half of this value.

7

The upwind TRB radial load had the largest disparity between the direct measurement and the models. The direct measurement was approximately 35 kN on average, and the analytic estimation was approximately 55 kN with a variation of ±20 kN. This variation was driven by the variation in the measured torque shown in Figure 2. Although the torque only varied by ±10% over each shaft revolution, the upwind TRB radial load was very sensitive to torque. The source of this consistent variation in torque is still being investigated. The SIMPACK model predicted that the upwind TRB was very lightly loaded, averaging approximately 15 kNm.

Finally, the highest correlation between the direct measurement and the models was found for the downwind TRB radial load. Here, all three methods averaged about 20 kN, with a variation of ±12 kN.
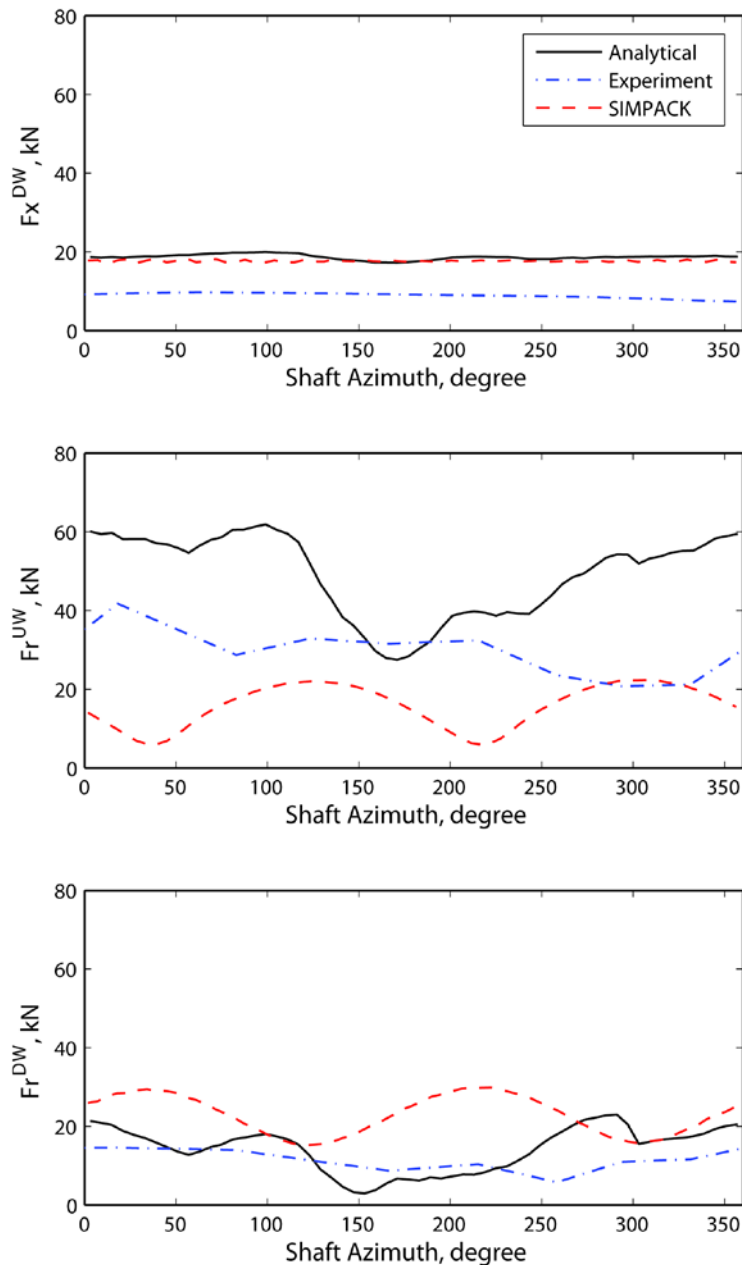

Figure 4. Comparison of directly measured, analytically inferred, and SIMPACK-predicted TRB

8

5 Conclusions

This work examined the loads on the HSS and TRBs of the GRC drivetrain at full-speed and full power. Experimental measurements of shaft bending and torque were compared to a SIMPACK multibody model. The global TRB loads were also calculated from direct experimental measurements of the load zone from instrumented slots on the TRB outer races, assuming a circular load zone distribution. Measured loads were compared to the global TRB loads predicted by the SIMPACK model and also to an estimation of the global TRB loads predicted by a simple, analytic model of the HSS that used measured shaft bending and torque as inputs. The analytic model was of interest because it could preclude the need for invasive instrumentation on the TRBs themselves and special calibration testing.

The measured shaft torque and bending moments compared favorably with the SIMPACK model, with the exception of the portion of the shaft downwind of the TRB pair. This section of the shaft was the most sensitive to assumptions regarding generator misalignment and generator coupling stiffness. In addition, the measured shaft torque displayed a variation of ±10% in magnitude very consistently over each revolution of the shaft. This variation was a primary contributor to nonconstant bearing loads; its source is still under investigation.

The directly measured global TRB loads compare favorably to SIMPACK model predictions and analytical model predictions for the downwind TRB axial and radial force, but disparities exist for the upwind TRB radial force.

Future work required to validate the analytical model will examine additional test cases for other steady state torque levels and intentional generator misalignment conditions. The source of the variation in torque signal is still being investigated as it plays a primary role in determining the bearing load zone. Additionally, load zone distributions other than circular will be investigated.

References

Link, H.; LaCava, W.; van Dam, J.; McNiff, B.; Sheng, S.; Wallen, R.; McDade, M.; Lambert, S.; Butterfield, S.; Oyague, F. (2011). "Gearbox Reliability Collaborative Project Report: Findings from Phase 1 and Phase 2 Testing." NREL/TP-5000-51885. Golden, CO: National Renewable Energy Laboratory, 88 pp.

Sheng, S. (2013). "Report on Wind Turbine Subsystem Reliability - A Survey of Various Databases." NREL/PR-5000-59111. Golden, CO: National Renewable Energy Laboratory, 43 pp.

Scott, K. G.; Infield, D.; Barltrop, N.; Coultate, J. K.; Shahaj, A. (2012). "Effects of extreme and transient loads on wind turbine drive trains." *50th AIAA Aerospace Sciences Meeting Including the New Horizons Forum and Aerospace Exposition*. AIAA; pp. 2012-1293.

Jain, S.; Hunt, H.E.M. (2011). "A dynamic model to predict the occurrence of skidding in wind-turbine bearings." *Journal of Physics: Conference Series 305*, IOP Publishing; doi:10.1088/1742-6596/305/1/012027.

Link, H.; Keller, J.; Guo, Y.; McNiff, B. (2012). "Gearbox Reliability Collaborative Phase 3 Gearbox 2 Test Plan." NREL/TP-5000-58190. Golden, CO: National Renewable Energy Laboratory, 105 pp.

Keller, J.; McNiff, B. (2014). "Gearbox Reliability Collaborative High-Speed Shaft Calibration." NREL/TP-5000-62373. Golden, CO: National Renewable Energy Laboratory, 31 pp.

Keller, J.; Guo, Y.; McNiff, B. (2013)."Gearbox Reliability Collaborative High Speed Shaft Tapered Roller Bearing Calibration." NREL/TP-5000-60319. Golden, CO: National Renewable Energy Laboratory, 34 pp.

Guo, Y.; Keller, J.; LaCava, W. (2014). "Planetary Gear Load Sharing of Wind Turbine Drivetrains Subjected to Non-Torque Loads." Wind Energy, doi: 10.1002/we.1731.